Unexpected role of ceruloplasmin in intestinal iron absorption

Srujana Cherukuri,[1,4] Ramesh Potla,[2,4] Joydeep Sarkar,[1,5] Saul Nurko,[3] Z. Leah Harris,[6] and Paul L. Fox[1,4,*]

[1]Department of Cell Biology, The Lerner Research Institute, Cleveland Clinic Foundation, Cleveland, Ohio 44195
[2]Department of Immunology, Cleveland Clinic Foundation, Cleveland, Ohio 44195
[3]Department of Nephrology and Hypertension, Cleveland Clinic Foundation, Cleveland, Ohio 44195
[4]Department of Biology, Cleveland State University, Cleveland, Ohio 44114
[5]Department of Biomedical Engineering, Case Western Reserve University, Cleveland, Ohio 44106
[6]Department of Anesthesiology, The Johns Hopkins School of Medicine, Baltimore, Maryland 21205
*Correspondence: foxp@ccf.org

Summary

Ferroxidases are essential for normal iron homeostasis in most organisms. The paralogous vertebrate ferroxidases ceruloplasmin (Cp) and hephaestin (Heph) are considered to have nonidentical functions in iron transport: plasma Cp drives iron transport from tissue stores while intestinal Heph facilitates iron absorption from the intestinal lumen. To clarify the function of Cp, we acutely bled $Cp^{-/-}$ mice to stress iron homeostasis pathways. Red cell hemoglobin recovery was defective in stressed $Cp^{-/-}$ mice, consistent with low iron availability. Contrary to expectations, iron was freely released from spleen and liver stores in $Cp^{-/-}$ mice, but intestinal iron absorption was markedly impaired. Phlebotomy of wild-type mice caused a striking shift of Cp from the duodenal epithelium to the underlying lamina propria, suggesting a critical function of Cp in basolateral iron transport. Regulated relocalization of intestinal Cp may represent a fail-safe mechanism in which Cp shares with Heph responsibility for iron absorption under stress.

Introduction

Iron is an essential cofactor of multiple proteins and enzymes, particularly those involving oxidation-reduction reactions and oxygen transport, but in excess it is highly toxic. Plasma iron homeostasis is maintained by stringent regulation of intestinal iron absorption and by release from tissues stores, primarily spleen and liver. Intestinal absorption of luminal nonheme iron is facilitated by a pathway centered on the duodenal enterocyte (Hentze et al., 2004). Dietary ferric ion in the lumen is reduced to ferrous ion at the apical surface of the cell; dcytB is a candidate ferrireductase (McKie et al., 2001), but a recent report indicates the possible participation of other, unidentified reductases (Gunshin et al., 2005). Ferrous ion is transported into the gut epithelium by divalent metal transporter-1 (DMT1) (Fleming et al., 1997; Gunshin et al., 1997). Basolateral release of epithelial iron is facilitated by the ferrous ion transporter ferroportin (Abboud and Haile, 2000; Donovan et al., 2000; McKie et al., 2000). The essential role of ferroportin in iron transport from enterocytes, as well as from macrophages and hepatocytes, has been demonstrated in ferroportin-deficient mice (Donovan et al., 2005).

The pathway taken by ferrous ion after leaving enterocytes remains uncertain, but it likely involves oxidation to ferric ion to increase binding to its carrier protein, transferrin. In vertebrates, ferrous ion oxidation is catalyzed by two copper-containing oxidases, ceruloplasmin (Cp) and hephaestin (Heph) (Chen et al., 2004; Osaki et al., 1966). Plasma Cp ferroxidase activity is thought to mobilize iron from tissue stores, particularly from reticuloendothelial macrophages (Osaki and Johnson, 1969). The important role of Cp in iron metabolism is most convincingly shown by iron accumulation in liver, brain, and other tissues in patients with aceruloplasminemia, an inherited Cp deficiency caused by *Cp* gene mutations. Iron overload in mice with targeted *Cp* gene deletion has confirmed the important role of Cp in iron homeostasis, and flux experiments with radiolabeled iron support the specific role of Cp ferroxidase activity in iron release from tissue stores (Harris et al., 2004, 1999). Cp is not thought to have a role in iron absorption since its transcript is not detected in the gastrointestinal tract (Aldred et al., 1987; Fleming and Gitlin, 1990; Klomp et al., 1996; Lockhart and Mercer, 1999), and because iron absorption is undiminished in $Cp^{-/-}$ mice (Harris et al., 1999; Yamamoto et al., 2002). Heph is a membrane-bound, Cp paralog with ferroxidase activity (Chen et al., 2004). *Heph* was discovered as the mutated gene responsible for the anemic phenotype in sex-linked anemia (sla) mice (Vulpe et al., 1999). Heph is abundant in the small intestine and is postulated to be responsible, in a couple with ferroportin, for basolateral iron transport from enterocytes (Chen et al., 2003). The differential tissue localization of Cp and Heph suggests they have different roles in iron homeostasis. However, the mild phenotype when either gene is inactivated, compared to the combined mutant mouse, suggests at least partial compensation of each ferroxidase by the other (Hahn et al., 2004).

Mechanisms are in place to rapidly up- or downregulate iron absorption and storage iron release in response to acute changes in iron requirements, for example, during erythropoietic demand for iron after blood loss. These mechanisms include transcriptional induction of proteins involved in iron transport e.g., dcytB, DMT1, and ferroportin (Fleming et al., 1997; McKie et al., 2001, 2000). Several of these proteins are also susceptible to iron-sensitive posttranscriptional regulatory mechanisms. Iron deficiency inhibits ferroportin mRNA translation by an iron-responsive element in its 5′UTR (Abboud and Haile, 2000; McKie et al., 2000). Ferroportin activity is down-

regulated by a unique posttranscriptional regulatory mechanism; excess iron induces liver secretion of hepcidin that binds to cell surface ferroportin and causes its internalization and degradation (Nemeth et al., 2004).

It is apparent from these examples that iron stress (either in deficit or excess) regulates iron homeostasis pathways at multiple steps and by multiple mechanisms. Moreover, application of stress is a powerful tool to unmask new functions of proteins, particularly in cases of partial genetic redundancy. To investigate the function of Cp, $Cp^{-/-}$ mice were subjected to acute blood removal to increase erythropoietic demand for iron. Unexpectedly, we have found that the primary function of Cp under stress is not to release iron from stores, but rather to increase iron absorption. Moreover, we find the mechanism of stress-mediated iron absorption involves a remarkable relocation of Cp from the cytosol of the duodenal epithelial cell to the underlying lamina propria. Here Cp may facilitate iron transport from ferroportin in the enterocyte basolateral membrane to transferrin for subsequent uptake by vessels in the villus interior.

Results

Defective recovery from acute bleeding in $Cp^{-/-}$ mice

$Cp^{-/-}$ and $Cp^{+/+}$ mice littermates were subjected to daily blood removal for 4 days to stress iron-related pathways. Before and during the bleeding period, blood hemoglobin was slightly lower in $Cp^{-/-}$ mice; however, hemoglobin recovery was substantially diminished in $Cp^{-/-}$ mice (Figure 1A). The hematocrit followed a similar pattern although the deficit in $Cp^{-/-}$ mice was less dramatic (Figure 1B). Serum iron was measured to determine the role of iron deficiency in defective hemoglobin recovery. As previously reported serum iron in $Cp^{-/-}$ mice is depressed (Cherukuri et al., 2004; Patel et al., 2002; Yamamoto et al., 2002), here about 35% of wild-type controls (Figure 1C). The early response of $Cp^{-/-}$ and $Cp^{+/+}$ mice to blood loss was nearly identical; a substantial increase in serum iron during the first 3 days was followed by a steep decline to a minimum at 5 days. A second phase of iron entry into blood was observed in $Cp^{+/+}$ mice and reached a maximum at about 7 days, however, this phase was entirely absent in $Cp^{-/-}$ mice (Figure 1C). In view of the ability of Cp ferroxidase activity to stimulate iron binding to transferrin (Sarkar et al., 2003), serum transferrin saturation was measured. The effect of phlebotomy on transferrin saturation was essentially identical to its effect on serum iron in both $Cp^{+/+}$ and $Cp^{-/-}$ mice (Figure 1D). The increase in transferrin saturation during the early phase after bleeding indicates that iron efficiently binds to transferrin even in the absence of Cp.

To determine whether the real-time presence of Cp was required for iron transport into plasma (versus the alternate requirement of Cp for previous development of the transport system), purified human Cp was injected into phlebotomized $Cp^{-/-}$ mice. In this experiment, phlebotomy more than doubled serum iron in $Cp^{+/+}$ mice to about 200 μg/dl, whereas serum iron in $Cp^{-/-}$ mice remained low after bleeding (Figure 1E). Injection of purified human Cp increased serum iron almost 10-fold. Parallel results were seen for transferrin saturation (Figure 1F). These results indicate that injected Cp can partially restore iron transport into plasma, and that there is a real-time requirement for Cp.

The source of the plasma iron was investigated by analysis of nonheme iron in storage tissues. The initial nonheme iron content of spleen in $Cp^{+/+}$ and $Cp^{-/-}$ mice was similar (Figure 1G). The steep drop in iron in both groups during the first five days suggests the spleen may be largely responsible for iron entry into plasma during the early response after blood loss. The decrease in liver iron was also similar in both mouse groups, but the rate of loss was an order-of-magnitude slower than in spleen (Figure 1H). Liver iron in $Cp^{-/-}$ mice before bleeding was substantially higher than in $Cp^{+/+}$ mice as previously reported (Cherukuri et al., 2004; Harris et al., 1999; Patel et al., 2002). The similar iron loss in $Cp^{+/+}$ and $Cp^{-/-}$ mice from both tissues suggests that differential iron release from stores is not responsible for the observed difference in serum iron accumulation during the late phase. Iron release from stores was confirmed histologically by Perl's staining of tissue slices. Substantial iron staining was seen in spleen of untreated $Cp^{+/+}$ (Figure 2A) and $Cp^{-/-}$ mice (Figure 2B), but iron was essentially absent after phlebotomy (Figure 2C shows $Cp^{-/-}$ mice, similar depletion of $Cp^{+/+}$ mice is not shown). Liver iron staining was much greater in $Cp^{-/-}$ mice (Figure 2F) than in $Cp^{+/+}$ mice (Figure 2E); bleeding partially decreased iron stain in $Cp^{-/-}$ mice (Figure 2G), confirming the chemical measurements. Our finding of iron release from spleen and liver of $Cp^{-/-}$ mice was unexpected in view of the proposed role of Cp in tissue iron release, and previous studies in $Cp^{-/-}$ mice showing defective iron release from the reticuloendothelial system (Harris et al., 2004, 1999). In previous mouse experiments, iron release was measured after infusion of damaged red blood cells where substantial newly delivered iron may be present in disequilibrium with storage pools. This intracellular labile iron pool is more susceptible to Cp-mediated efflux compared to iron in the storage pool, e.g., bound to ferritin (Sarkar et al., 2003). In contrast, here we measure tissue release of endogenous iron stores, and under stress conditions of acute blood loss.

Role of Cp in stress-induced iron absorption

Because tissue iron release was not impaired, we considered the possibility that decreased intestinal iron absorption was responsible for the absent second phase of plasma iron entry and diminished hemoglobin formation in $Cp^{-/-}$ mice. Phlebotomized mice were placed on an iron-deficient diet immediately after the first bleed. The early increase in serum iron in both mouse groups was as before; however, the second phase of iron entry was greatly diminished in $Cp^{+/+}$ mice (Figure 3A), as was the increase in transferrin saturation (Figure 3B). The combined stress of phlebotomy and an iron-deficient diet would be expected to induce more pronounced iron release from tissues to sustain erythropoiesis. Rapid and complete release of nonheme iron from spleen was observed in $Cp^{+/+}$ and $Cp^{-/-}$ mice (Figure 3C); however, the depletion rate was similar to that of iron-sufficient mice. In marked contrast to the result in bled, iron-sufficient mice, application of the dual stress to $Cp^{-/-}$ mice induced a dramatic decrease in liver nonheme iron (Figure 3D). Tissue iron depletion in $Cp^{-/-}$ mice during dietary iron-deficiency was confirmed histologically in spleen (Figure 2D) and liver (Figure 2H), and confirms tissue iron release even in the absence of Cp.

The absence of the second recovery phase in mice fed an iron-deficient diet suggests that plasma iron in this phase is derived primarily from the diet. As a corollary, since this phase

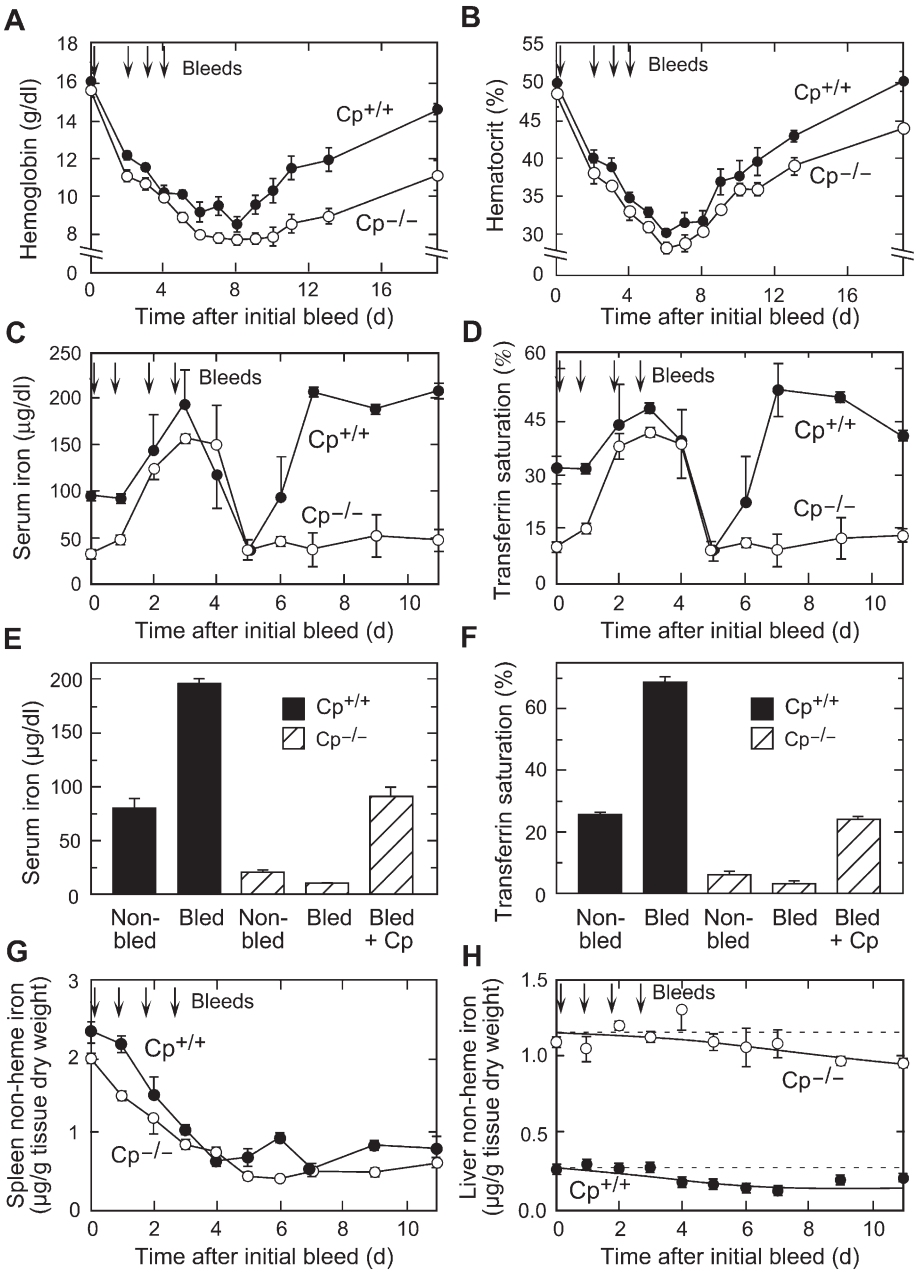

Figure 1. Defective erythropoietic recovery of $Cp^{-/-}$ mice after acute bleeding

$Cp^{-/-}$ (o) and $Cp^{+/+}$ (•) mice were subjected to acute bleeding stress by withdrawal of 300–350 µl of blood from the retro-orbital plexus on each of 4 days (indicated by arrows). On succeeding days blood samples (about 60 µl) were withdrawn and hemoglobin (**A**) and hematocrit (**B**) were measured and expressed as mean ± SEM (six mice per group). The role of Cp in regulating iron entry into plasma was determined. Mice (six mice per group at each time) were sacrificed at intervals and serum iron (**C**) and transferrin saturation (**D**) were determined. In a separate experiment, 7 days after initiation of bleeding $Cp^{+/+}$ (black bars) and $Cp^{-/-}$ (striped bars) mice, $Cp^{-/-}$ mice were injected intraperitoneally with purified human Cp (6 µg/100 µl of circulating blood volume). After 24 hr, serum iron (**E**) and transferrin saturation (**F**) were determined. Nonheme iron in liver (**G**) and spleen (**H**) of phlebotomized mice were measured using bathophenanthroline, and expressed as mean ± SEM (dashed line shows initial value).

is also absent in $Cp^{-/-}$ mice on an iron-sufficient diet, Cp may be required for intestinal iron absorption. Intestinal absorption was measured directly by gavage with ^{59}Fe (Ajioka et al., 2002). As previously reported (Harris et al., 1999; Yamamoto et al., 2002), gut iron absorption was the same in nonbled, $Cp^{+/+}$ and $Cp^{-/-}$ mice: about 11% of administered iron in 24 hr (Figure 3E). Phlebotomy increased absorption by almost 5-fold in $Cp^{+/+}$ mice, but the response was substantially blunted in $Cp^{-/-}$ mice. To distinguish between a defect in mucosal iron uptake versus iron transfer to the portal circulation, intestinal ^{59}Fe was measured. In bled mice, intestinal ^{59}Fe was more than two times higher in $Cp^{-/-}$ mice than in wild-type controls indicating that Cp does not influence iron uptake into the gut, but instead facilitates release of iron from absorptive epithelial cells into the circulation (Figure 3F).

In vivo expression and stress-induced relocalization of Cp

To gain insight into the function of Cp in phlebotomy-stimulated iron absorption, we investigated the effect of acute bleeding on Cp expression. Cp mRNA expression in liver, the primary source of circulating Cp, was measured by Northern analysis. Hepatic Cp mRNA was not altered during the 10 day period after bleeding was initiated (Figure 4A). Similarly, immunoblot analysis showed that plasma Cp concentration was unchanged (Figure 4B). Cp mRNA is not expressed in the gastro-

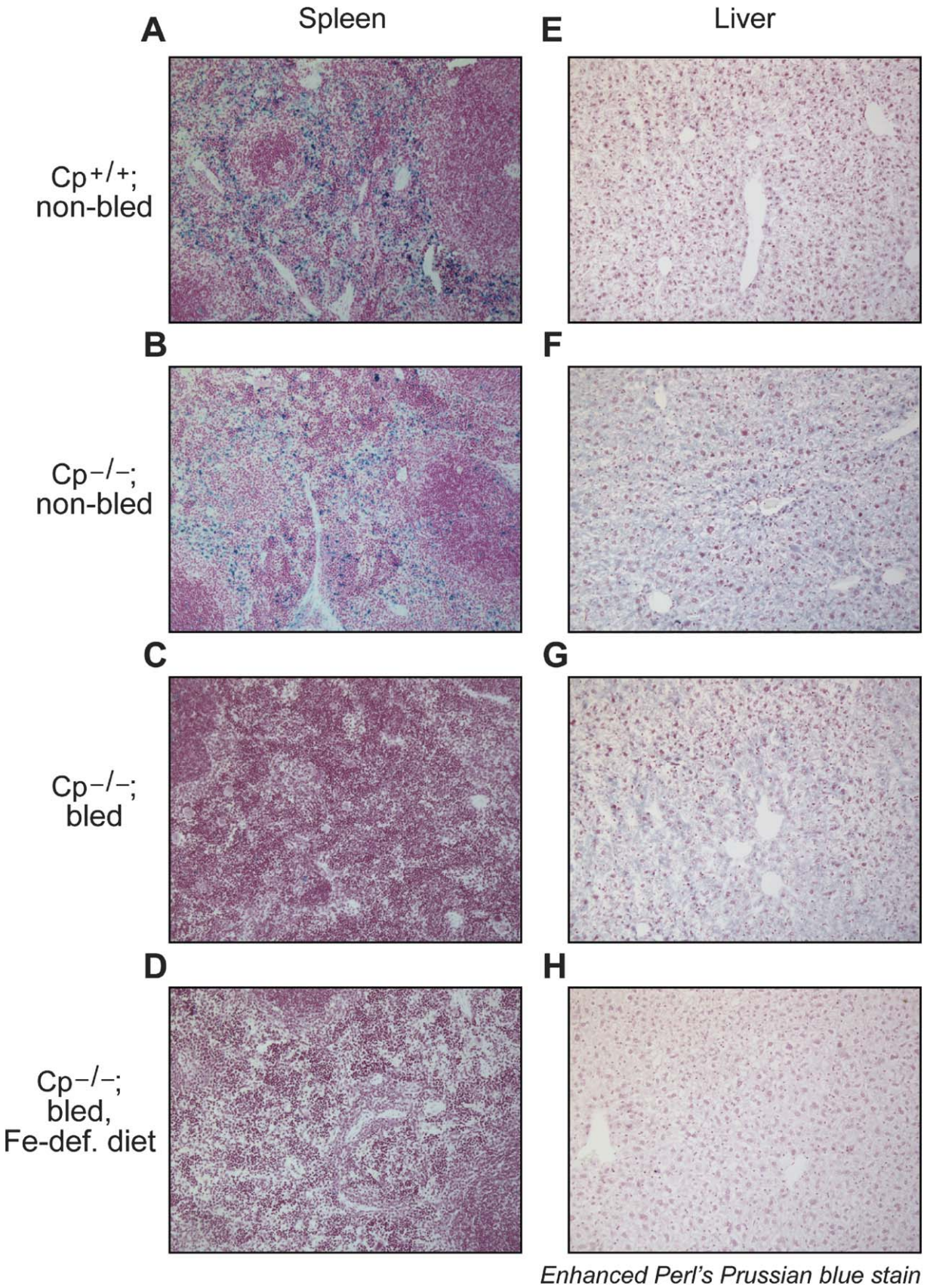

Figure 2. Depletion of tissue iron stores in $Cp^{-/-}$ and $Cp^{+/+}$ mice subjected to stress

Iron in spleen (left panels) and liver (right panels) was detected by enhanced Perl's Prussian blue stain; nonbled $Cp^{+/+}$ (**A** and **E**) and $Cp^{-/-}$ (**B** and **F**) mice were compared. Tissue iron was measured in $Cp^{-/-}$ mice subjected to acute bleeding stress 7 days after initiation of bleeding (**C** and **G**), and in mice subjected to acute bleeding stress and an iron-deficient (Fe-def.) diet 10 days after initiation of bleeding (**D** and **H**). Staining is representative of four mice in each group.

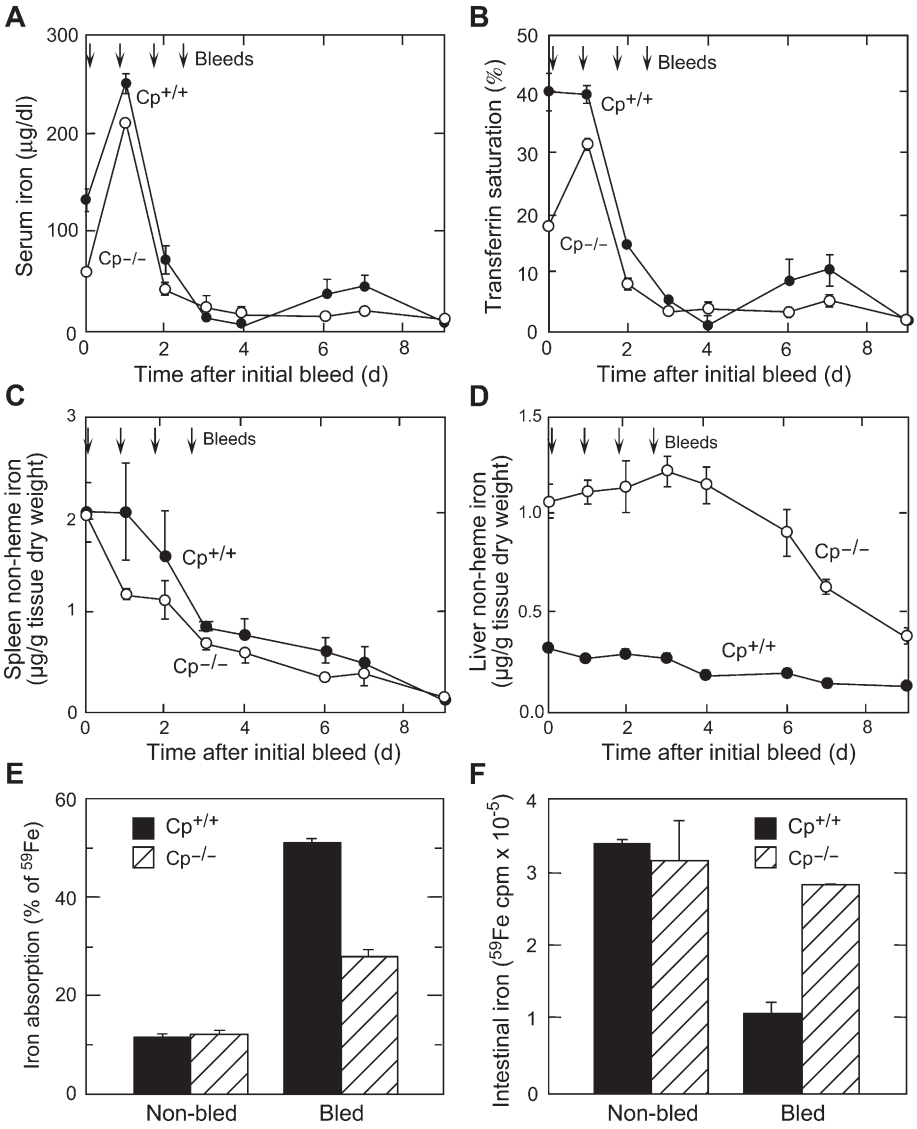

Figure 3. Important role of Cp in stress-induced iron absorption

$Cp^{-/-}$ (o) and $Cp^{+/+}$ (•) mice were bled on four consecutive days (indicated by arrows). The mice were placed on an iron-deficient diet immediately after the first bleed and maintained on the diet until sacrifice. Serum iron (**A**) and transferrin saturation (**B**) were measured and expressed as mean ± SEM (seven mice per group at each time point). Spleen **(C)** and liver **(D)** nonheme iron was measured using bathophenanthroline. In a separate experiment, ^{59}Fe was administered by gavage to control and acutely bled $Cp^{-/-}$ (striped bars) and $Cp^{+/+}$ (black bars) mice. Iron absorption (**E**) was determined as the sum of radioactivity in blood, organs, and carcass, and expressed as percent of administered ^{59}Fe. ^{59}Fe retained in the small intestine (**F**) was determined separately. Results are expressed as mean ± SEM (six mice per group).

intestinal tract (Aldred et al., 1987; Fleming and Gitlin, 1990; Klomp et al., 1996; Lockhart and Mercer, 1999), but our finding that Cp facilitates iron absorption suggests that the expressed protein may be present. Furthermore, the specific need for Cp after bleeding suggests that Cp may be induced or activated by the stress. Immunoblot analysis revealed that Cp protein was in fact abundant in lysates of proximal duodenum of $Cp^{+/+}$ mice, but the level was not increased by phlebotomy (Figure 4C). Consistent with previous reports, Cp mRNA was not detected in duodenal tissue by Northern analysis (Figure 4D) or by RT-PCR (data not shown).

We considered the possibility of a compensatory increase in Heph expression in the gut of $Cp^{-/-}$ mice (although this increase would not account for decreased absorption in the mice). Northern analysis of proximal duodenum did not show altered expression of Heph in $Cp^{-/-}$ mice (Figure 4E), a result consistent with a previous result in independently generated $Cp^{-/-}$ mice on a mixed-strain background (Yamamoto et al., 2002). In view of the important function of hepcidin as a negative regulator of iron absorption, we also considered the possibility that decreased absorption in $Cp^{-/-}$ mice reflects altered liver hepcidin expression. Northern analysis of liver extracts indicates that hepcidin mRNA in nonbled $Cp^{-/-}$ mice is about half that of $Cp^{+/+}$ mice (Figure 4F), consistent with its state of moderate anemia. If altered hepcidin expression is responsible for the differential absorption in these mice, we would expect relatively higher absorption in $Cp^{-/-}$ mice, in contrast to our results. Also, our finding that phlebotomized $Cp^{-/-}$ mice exhibit impaired iron absorption, but not defective iron release from spleen or liver, is not consistent with a primary role of hepcidin since the hormone decreases ferroportin-mediated iron release from all of these tissues (Donovan et al., 2005; Nemeth et al., 2004). Together, these results indicate that altered hepcidin expression by itself is unlikely to explain the defective absorption in $Cp^{-/-}$ mice, and that Cp likely mediates a metabolic step downstream of hepcidin.

Immunofluorescence labeling of transverse sections of proximal duodenum from wild-type mice revealed abundant Cp in

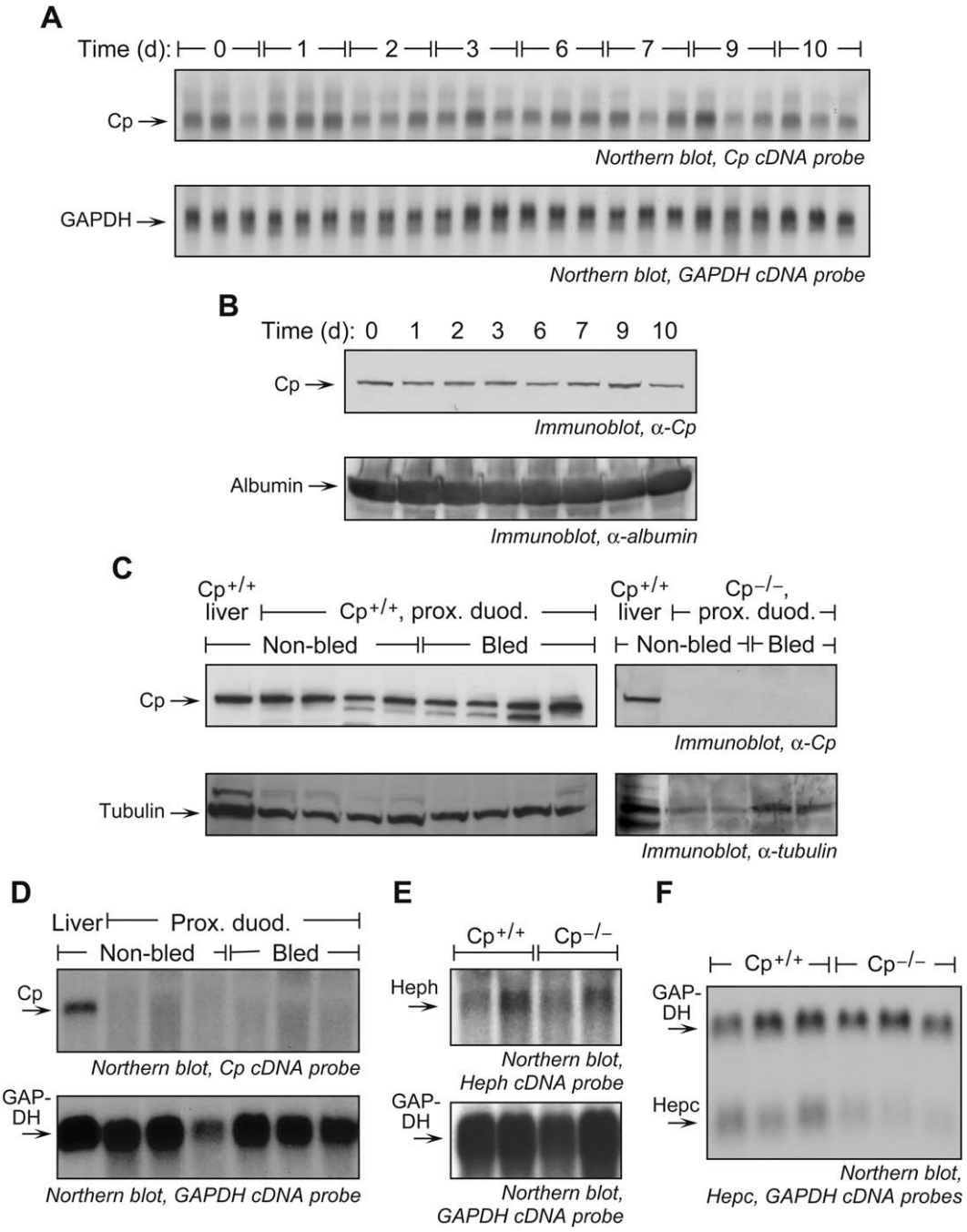

Figure 4. Cp protein but not mRNA is expressed in mouse duodenum

$Cp^{+/+}$ mice were bled on 4 consecutive days and sacrificed at intervals.

A) mRNA was isolated from liver (n = 3 mice) and subjected to 1% agarose gel electrophoresis and Northern analysis with random-primer, ^{32}P-labeled cDNA probes against human Cp (upper panel) and GAPDH (lower panel).

B) Plasma samples (n = 4 mice) were subjected to SDS-PAGE and immunoblot analysis using rabbit anti-Cp (upper panel) and mouse anti-albumin (lower panel) antibodies.

C) Proximal duodenum (prox. duod.) extracts from $Cp^{+/+}$ (left panels) and $Cp^{-/-}$ mice (right panels) were subjected to SDS-PAGE and immunoblot analysis using rabbit anti-Cp (upper panel) and mouse anti-tubulin (lower panel) antibodies. A liver extract from a $Cp^{+/+}$ mouse served as a positive control. In a separate experiment, $Cp^{+/+}$ and $Cp^{-/-}$ mice were bled four times as above. Seven days after the initial bleed, mice were sacrificed and the proximal duodenum was collected and homogenized.

D) RNA was isolated from proximal duodenum from control and bled $Cp^{+/+}$ mice and subjected to 1% agarose gel electrophoresis and. RNA isolated from $Cp^{+/+}$ mouse liver served as a positive control.

E) RNA isolated from proximal duodenum from nonbled mice was subjected to Northern analysis with ^{32}P-labeled cDNA probes against human Heph (upper panel) and human GAPDH (lower panel).

F) RNA isolated from liver from nonbled mice was subjected to Northern analysis with ^{32}P-labeled human GAPDH (above) and mouse hepcidin (Hepc, below) cDNA probes.

enterocyte cytoplasm, predominantly in the supranuclear region lining the gut lumen (Figure 5A). The low amount of Cp in the lamina propria of the villus interior was unexpected in view of evidence that iron release from cells is facilitated by extracellular Cp (Osaki and Johnson, 1969; Sarkar et al., 2003). After phlebotomy, Cp in the villus interior dramatically increased at the expense of enterocyte Cp; densitometric analysis indicated about a 2.5-fold increase in lamina propria Cp concentration and about a one-third decrease in enterocyte Cp. Immunohistochemical analysis of lateral sections of duodenum showed a similar relocation of Cp along the entire villus length (Figure 5B). As a control, glyceraldehyde 3-phosphate dehydrogenase did not exhibit bleeding-induced relocalization, indicating target protein specificity (Figure 5C). The relocalization of Cp to the lamina propria is consistent with a role for Cp in iron release from the basolateral aspect of the duodenal epithelium during conditions of stress requiring high iron absorption.

The presence of Cp in the duodenum, despite the absence of its transcript, suggests that gut Cp is derived from another tissue, most likely the liver, and transported via the blood. We tested this possibility by intravenous injection of mouse Cp (from $Cp^{+/+}$ mouse serum) into $Cp^{-/-}$ mice. After 24 hr, abundant Cp was observed by immunofluorescence in duodenal epithelial cells with an intracellular distribution similar to that seen in nonbled, wild-type mice (Figure 5D, left). Similar results were observed after injection of serum that was albumin-depleted to reduce the amount of injected protein (Figure 5D, center) or purified human Cp (data not shown). In a control, Cp was undetectable in $Cp^{-/-}$ mice not injected with exogenous Cp (Figure 5D, right).

Discussion

The specific functions of ferroxidases in intestinal iron absorption are not yet clear. Heph, a membrane-bound Cp paralog, has been implicated as the critical ferroxidase in iron absorption since the protein is abundant in duodenum and the gene is mutated in the *sla* mouse which has defective iron absorption (Chen et al., 2004; Vulpe et al., 1999). Most Heph protein is localized in vesicles within the enterocyte (Frazer et al., 2001), but some may be present on the basolateral membrane (Kuo et al., 2004). Based on our measurements of iron absorption, and on the assumption that Cp in the villus interior is functional in absorption, we can estimate the relative iron flux through Cp-dependent and Cp-independent pathways. We propose the following model (which makes the additional assumption that the Cp-independent pathway is Heph dependent): In the nonbled, wild-type mouse (Figure 6A), Fe^{3+} from the duodenal lumen is reduced by Dcytb (or other reductases) to Fe^{2+}, which traverses the enterocyte apical membrane via DMT1. Intracellular iron is transported by as-yet undefined processes, possibly within vesicles. Estimation of the kinetic parameters by nonlinear regression analysis (Dennis et al., 1981) suggests that under basal conditions, in which approximately 10% of the applied iron is absorbed, about 3/4 utilizes the Heph-dependent pathway while the remaining 1/4 is Cp dependent. Extracellular Cp may act in tandem with ferroportin, an iron transporter spanning the basolateral membrane of duodenal epithelium (Abboud and Haile, 2000; Donovan et al., 2000; McKie et al., 2000). According to one possible mechanism, extracellular Cp ferroxidase activity converts newly exported ferrous ion to ferric ion for binding to transferrin and subsequent uptake by transferrin receptors on vessels within the villus interior. In bled mice (Figure 6B), iron deficiency markedly induces Dcytb and DMT1 expression (Dupic et al., 2002) and enterocyte iron uptake is correspondingly increased, in our experiment by almost 5-fold to about 50% of ingested iron. According to our model, blood loss induces Cp relocalization to the sub-epithelial space, and iron flux is evenly divided between the Cp-dependent pathway and Heph-dependent pathways. It may be noted that our flux estimates are model dependent, and it is possible that the Cp-dependent pathway becomes significant only after stress exceeds the capacity of the Heph-dependent pathway.

The absence of Cp mRNA in the duodenum was consistent with previous reports (Aldred et al., 1987; Fleming and Gitlin, 1990; Klomp et al., 1996; Lockhart and Mercer, 1999), but the finding of Cp protein in duodenal epithelial cells was unexpected. Liver-derived Cp from the plasma is the likely source of intestinal Cp since intravenous injection of human or mouse Cp resulted in uptake and accumulation in duodenal epithelial cells. High-affinity cell surface Cp receptors have been reported on liver endothelial cells and Kupffer cells (Dini et al., 1990; Tavassoli et al., 1986), thus the pathway of Cp entry may involve receptor-mediated endocytosis and localization in intracellular vesicles. However, Cp receptors on intestinal epithelial cells have not been described. The mechanism underlying phlebotomy-induced relocalization of Cp to the lamina propria is not understood; it may involve regulated release of Cp from the enterocyte, or alternatively, inhibited enterocyte uptake from plasma. The function of Cp within the enterocyte is likewise unclear. Intracellular Cp may have a role in iron trafficking across the enterocyte. Alternatively, Cp participation in host defense is suggested by in vitro evidence of bactericidal activity (Klebanoff, 1992), and by our finding of abundant Cp in the colon, a site not involved in iron absorption (data not shown). Cp's contribution to iron absorption may explain the curious developmental phenotype of the *sla* mouse, i.e., severe anemia at birth that normalizes during maturation (Bannerman and Cooper, 1966). Hepatic Cp mRNA expression (and plasma Cp) follows a similar pattern, low expression at birth and increasing until adulthood (Fleming and Gitlin, 1990). Thus, the combination of defective Heph and low intestinal Cp may be responsible for severe anemia in young *sla* mouse which yields as Cp increases during development. The shared responsibility of the two related ferroxidases in absorption may have evolved as a fail-safe mechanism to ensure iron availability under stress.

Our results may have practical implications regarding the rational treatment of aceruloplasminemia. Serial phlebotomy of a single aceruloplasminemia patient failed to deplete hepatic iron, leading the authors to conclude that tissue iron stores can not be depleted in the absence of Cp (Hellman et al., 2000). Our results indicate that phlebotomy induces iron release from storage sites even in the absence of Cp. Both spleen and liver iron in $Cp^{-/-}$ mice are depleted by bleeding, but iron is depleted from liver at a substantially slower rate than from spleen. However, substitution of an iron-deficient diet to phlebotomized mice causes rapid and near-complete iron release from liver as well as from spleen. In addition to the difference in dietary iron, there are other important differences between our study on mice and the treatment of the patient. For one, the mice were otherwise healthy, young adults, whereas the patient

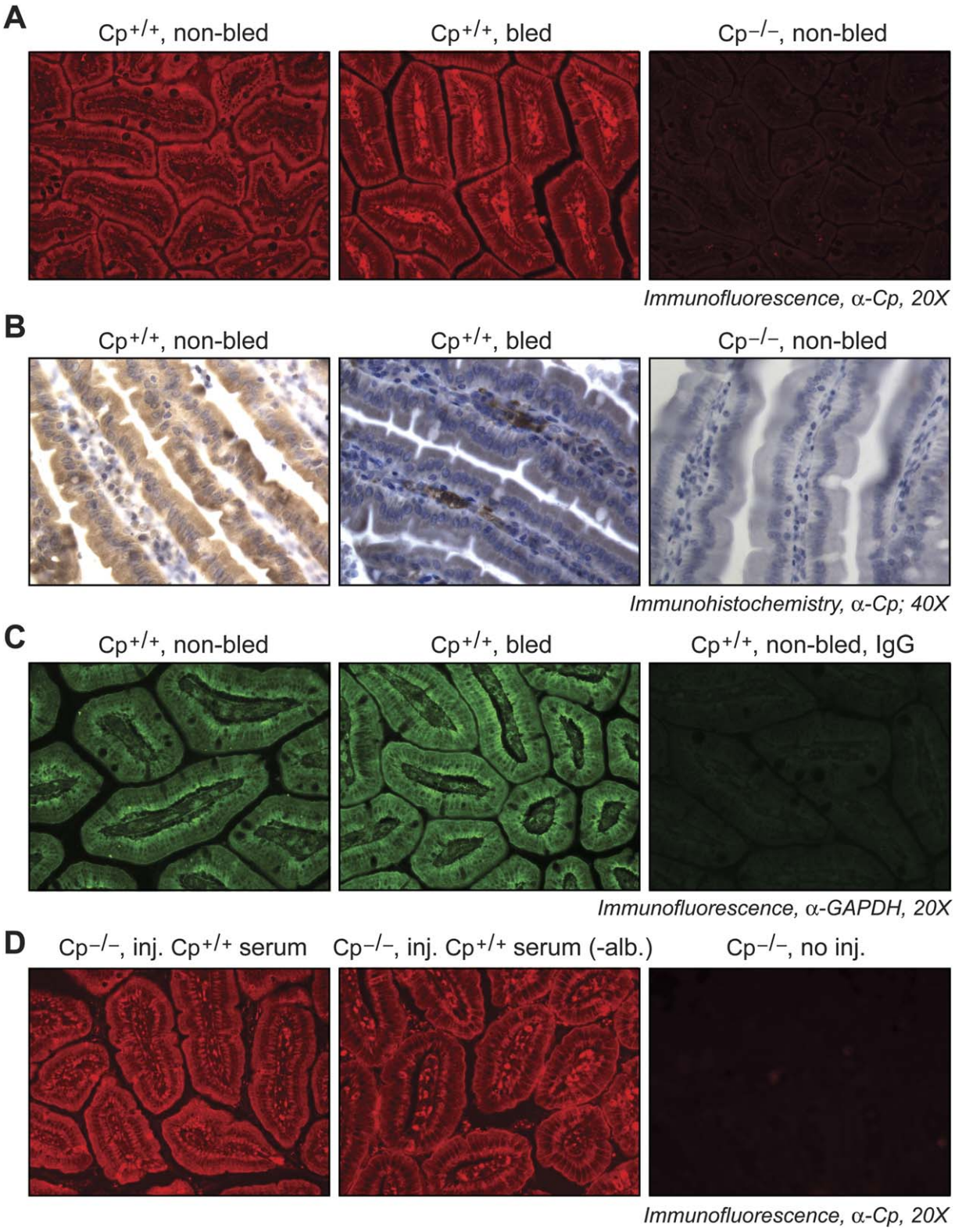

Figure 5. Cp entry into mouse duodenum and relocalization after bleeding stress

$Cp^{+/+}$ mice were phlebotomized on four consecutive days and sacrificed 7 days after initiation of bleeding.

A) Transverse sections of proximal duodenum of nonbled (left) and bled (center) $Cp^{+/+}$ mice were subjected to immunofluorescence microscopy using rabbit anti-human Cp antibody. Nonbled $Cp^{-/-}$ mice were used as control for antibody specificity (right).

B) Lateral sections of proximal duodenum of nonbled (left) and bled (center) $Cp^{+/+}$ mice were subjected to immunohistochemical analysis using rabbit anti-Cp antibody. Nonbled $Cp^{-/-}$ mice were used as control for antibody specificity (right).

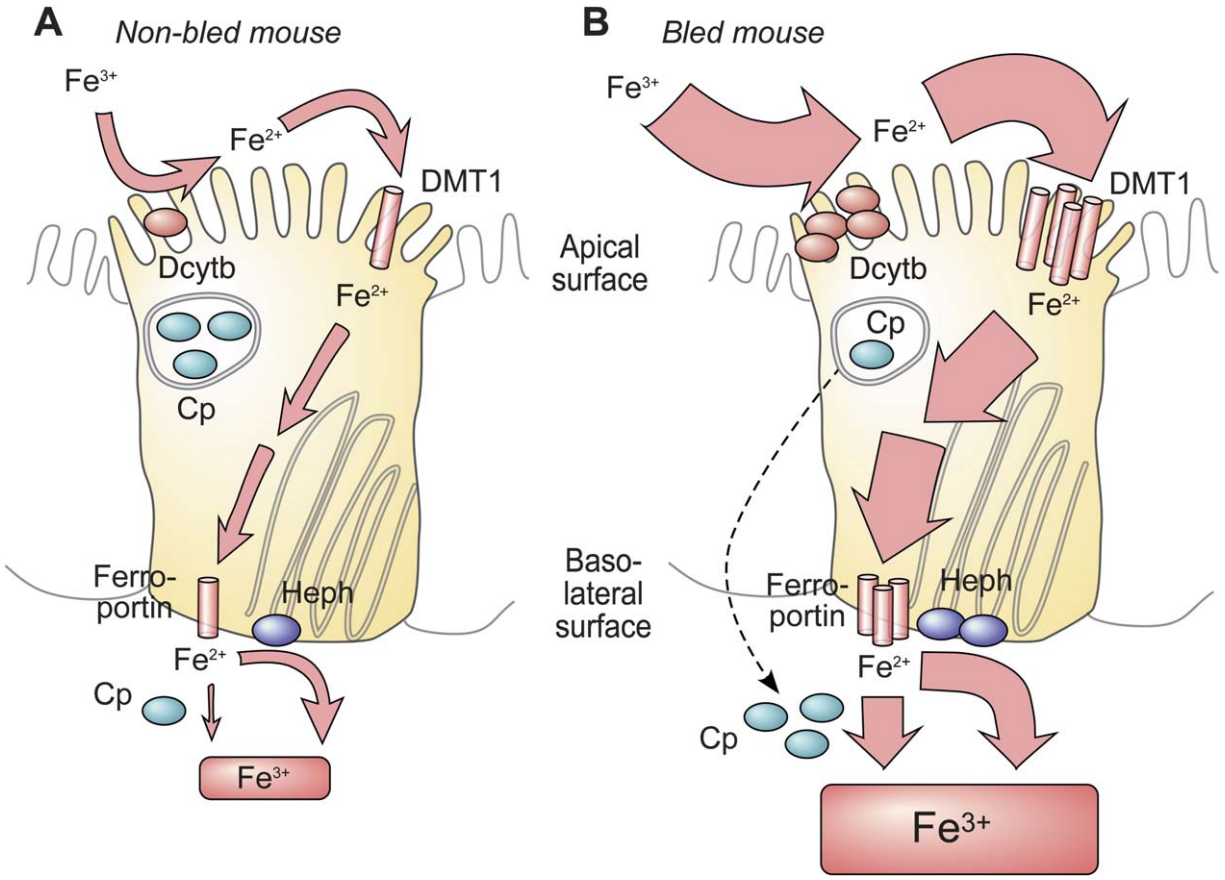

Figure 6. A dual ferroxidase system contributes to iron absorption

Iron absorption by $Cp^{-/-}$ and $Cp^{+/+}$ mice as determined by gavage, and relative levels of Cp in lamina propria of bled and nonbled mice, were used to estimate iron flux through Cp-dependent and Cp-independent (most likely, Heph-mediated) pathways. Solid arrows represent individual pathway steps; the width is proportional to the flux estimated using exponential models. The probable localization of Cp in intracellular vesicles is indicated. NL2SOL was used for parameter estimation by adaptive nonlinear least square error estimation (Dennis et al., 1981), and LSODES was used for solving the simultaneous differential equations. Relative roles of Cp and Heph in iron absorption are shown for nonbled (**A**) and bled mice (**B**). Cp relocalization is indicated by dashed line.

was a diabetic 52-year-old. Also, our mouse-bleeding regimen was very severe, removing 20% of blood volume per day compared to removal of 5% of blood volume per week from the patient. Finally, there may be differences between iron storage and release mechanisms between mice and humans. Future mouse experiments may lead to the development of a tolerable, long-term treatment regimen combining mild phlebotomy with an iron-deficient diet, which would reduce tissue iron load and improve the quality and duration of life in patients.

Experimental procedures

Mice

Mice with targeted Cp gene deletion (Harris et al., 1999) were backcrossed for 9 to 11 generations into the C57BL/6J background. $Cp^{-/-}$ and $Cp^{+/+}$ littermates (10- to 12-week-old males) that were progeny of $Cp^{+/-}$ crosses were used in all experiments. To induce erythropoietic stress, mice were subjected to acute bleeding by withdrawal of 300 to 350 μl of blood per day from the retro-orbital plexus for four consecutive days. All studies followed a protocol approved by the Animal Review Committee of the Cleveland Clinic Foundation.

Blood collection and determination of blood hemoglobin and hematocrit

Blood (about 60 μl) was obtained by insertion of a heparin-coated capillary tube into the retro-orbital plexus. The hematocrit, a measure of efficiency of erythropoiesis, was determined by centrifugation of sample in capillary tube. Total blood hemoglobin, which reflects both erythropoietic efficiency as well as marrow iron status, was determined by a colorimetric method specific for cyanmethemoglobin (Sigma Diagnostics). To prepare serum for injection into mice, blood from wild-type, C57Bl/6J mice was collected by

C) Transverse sections of proximal duodenum of untreated (left) and bled (center) $Cp^{+/+}$ mice were subjected to immunofluorescence microscopy using mouse monoclonal anti-rabbit GAPDH primary antibody. Mouse IgG primary antibody was used as control for specificity (right).

D) To determine whether intestinal Cp is derived from blood, 200 μl of whole serum (left) or albumin-depleted serum (-alb., center) from $Cp^{+/+}$ mice was injected (inj.) into the tail vein of nonbled, $Cp^{-/-}$ mice. Uninjected $Cp^{-/-}$ mice served as controls (right). After 24 hr, proximal duodenum was collected, and transverse sections were subjected to immunofluorescence using rabbit anti-Cp antibody.

cardiac puncture, and serum was separated by centrifugation at 5000 rpm for 5 min. Albumin was removed from serum using Montage albumin deplete kit (Millipore, Denver, Massachusetts). Albumin-depleted serum was dialyzed overnight at 4°C against phosphate-buffered saline (PBS) in 10,000 kDa cut-off dialysis cassettes (Slide-A-Lyzer, Pierce, Rockford, Illinois).

Determination of serum and tissue iron

Blood (about 500 μl) was collected at sacrifice by cardiac puncture using 1-ml syringe with 26-gauge needle, and serum was obtained by centrifugation at 5,000 rpm for 5 min. Serum iron and total iron binding capacity (TIBC) were determined by a kit (Stanbio). Transferrin saturation was calculated as (serum iron ÷ total iron binding capacity) × 100%. Nonheme iron in liver and spleen was measured by the bathophenanthroline method and the results expressed as μg of iron per g of tissue dry weight (Torrance and Bothwell, 1980). For histological determination of tissue iron stores, liver and spleen were fixed in 10% phosphate-buffered formalin and were embedded in paraffin. The sections were dehydrated in xylene and by an ethanol-water series (100%, 90%, 75%, 50%) and stained with Perl's Prussian blue stain and counterstained with pararosaniline (Sigma). Stained sections were dehydrated by an ethanol and xylene series, and mounted in Permount.

Determination of intestinal iron absorption

Iron absorption was measured after gavage with ^{59}Fe as described (Ajioka et al., 2002). Briefly, 7 days after initiation of bleeding, control and phlebotomized mice were fasted overnight. ^{59}Fe-HCl (2.5 μCi) in 0.2 ml of a solution containing 0.5 M ascorbic acid, 0.15 M NaCl, and $FeSO_4$ (5 μg of total iron) was administered orally with an olive-tipped gavage needle. The mice were placed in metabolic cages, fasted for another 7 hr, and then chow was restored. Mice were sacrificed 24 hr after gavage. Lungs, head, and the gastrointestinal tract were removed for separate counting, and radioactivity in blood, major organs, and carcass was analyzed by γ-counter. Percent of iron absorbed was calculated as 100 × (^{59}Fe in blood, organs, and carcass ÷ ^{59}Fe administered by gavage).

Immunolocalization of Cp in mouse duodenum

The proximal duodenum from $Cp^{-/-}$ and $Cp^{+/+}$ mice was washed in ice-cold PBS and fixed in Bouin's fixative for 12–14 hr. The fixed tissues were washed in 70% ethanol, dehydrated by a series of ethanol and xylene rinses, and embedded in paraffin. For immunofluorescence, 5-μm sections were de-paraffinized in xylene, and rehydrated in a series of 100%, 90%, 80%, and 50% ethanol, water, and PBS. The sections were pressure-cooked in 10 mM citric acid buffer for antigen retrieval. Antigen-retrieved sections were blocked with PBS containing 3% bovine serum albumin and 0.2% Triton X-100 for 30 min at 37°C. The sections were incubated overnight at 4°C with rabbit anti-human Cp antibody (Accurate, 1:200). Sections were washed with 0.05% Triton X-100 and 0.7% fish skin gelatin in PBS, and incubated with Alexa Fluor 568 goat anti-rabbit IgG (Molecular Probes) as a secondary antibody for 1 hr at 37°C. Sections were washed and mounted with Vectashield mounting medium (Vector).

For immunohistochemistry, sections were dehydrated and antigen-retrieved. Sections were stained using an automated system (ES Autostainer) and a DAB detection kit (Ventana). Nonspecific binding was reduced using an avidin/biotin blocking kit (Ventana). Rabbit anti-human Cp was used as primary antibody (Accurate, 1:200) and goat anti-rabbit IgG conjugated to biotin as secondary antibody, and the avidin-biotin complex was detected with horseradish peroxidase. Slides were counterstained with hematoxylin, dehydrated in ethanol and cleared in xylene, and mounted in Permount.

Immunoblot analysis of mouse tissue

Mouse proximal duodenum was washed in ice-cold PBS and snap-frozen in liquid N_2. The tissue was homogenized in 50 mM Tris-HCl (pH. 7.4), 1% Triton X-100, 1 mM EDTA, 1 mM PMSF, 5 μg/ml aprotinin, 1 μg/ml pepstatin, 2 μg/ml leupeptin, 1 mM sodium orthovanadate, and 1 mM NaF. Lysates were incubated on ice for 30 min, centrifuged at high speed for 10 min, and supernatant protein determined by Bio-Rad assay. Lysates (100 μg of protein) were subjected to 10% SDS-PAGE and transferred to an immobilion-P membrane (Millipore, Bedford, MA). The membrane was probed with rabbit anti-human Cp as antibody (Accurate, 1:5,000) and then with peroxidase-conjugated anti-rabbit IgG as secondary antibody (1:10,000). Cp was detected by chemiluminescence (ECL-plus, Amersham). The membrane was stripped and reprobed with mouse anti-human tubulin (Oncogene, 1:5,000) antibody followed by peroxidase-conjugated anti-mouse IgG (1:10,000).

Northern blot analysis of mouse tissue

Mouse proximal duodenum and liver were washed in ice-cold PBS and snap-frozen in liquid N_2. Tissue was homogenized in Trizol reagent and RNA was isolated. RNA (10 μg total RNA) was subjected to electrophoresis on a formaldehyde-agarose gel and transferred to Hybond-N nitrocellulose membrane (Amersham). RNA was UV-crosslinked and hybridized with ^{32}P-labeled mouse Cp (forward primer, 5′-TTTCCCCACCCATAGCTCTGTC-3′; reverse primer, 5′-CTTGCCCTTCCCTCACATA-CCA-3′), mouse hepcidin (forward primer, 5′-AGAAAGCAGGGCAGACATTGC-3′; reverse primer, 5′-TTCAAGGTCATTGGTGGGGAG-3′), or mouse GAPDH (forward primer, 5′-TGTTCCAGTATGACTCCACTCACG-3′; reverse primer, 5′-AGATGATGACC-CGTTTGGCTC-3′) cDNA probes prepared by random primer labeling (Amersham). ^{32}P-labeled probe corresponding to nucleotide positions 1000-2200 of the human Heph ORF was prepared by RT-PCR of the full-length cDNA.

Statistical analysis

A minimum of six mice in each group was analyzed for all experiments, unless otherwise specified. The results were expressed as mean ± standard error of mean (SEM). Statistical analysis was done by Student's t test using GraphPad Prism software.

Acknowledgments

This work was supported by National Institutes of Health grants P01 HL29582, R01 HL67725, P01 HL76491 (to P.L.F.), R01 DK58086 (to Z.L.H.), and K08 DK65670 (to S.N.), and by a Graduate Student Fellowship Award from the American Heart Association, Ohio Valley (to S.C.).

Received: March 20, 2005
Revised: July 10, 2005
Accepted: October 12, 2005
Published: November 8, 2005

References

Abboud, S., and Haile, D.J. (2000). A novel mammalian iron-regulated protein involved in intracellular iron metabolism. J. Biol. Chem. *275*, 19906–19912.

Ajioka, R.S., Levy, J.E., Andrews, N.C., and Kushner, J.P. (2002). Regulation of iron absorption in *Hfe* mutant mice. Blood *100*, 1465–1469.

Aldred, A.R., Grimes, A., Schreiber, G., and Mercer, J.F. (1987). Rat ceruloplasmin. Molecular cloning and gene expression in liver, choroid plexus, yolk sac, placenta, and testis. J. Biol. Chem. *262*, 2875–2878.

Bannerman, R.M., and Cooper, R.G. (1966). Sex-linked anemia: A hypochromic anemia of mice. Science *151*, 581–582.

Chen, H., Attieh, Z.K., Su, T., Syed, B.A., Gao, H., Alaeddine, R.M., Fox, T.C., Usta, J., Naylor, C.E., Evans, R.W., et al. (2004). Hephaestin is a ferroxidase that maintains partial activity in *sex-linked anemia* mice. Blood *103*, 3933–3939.

Chen, H., Su, T., Attieh, Z.K., Fox, T.C., McKie, A.T., Anderson, G.J., and Vulpe, C.D. (2003). Systemic regulation of Hephaestin and Ireg1 revealed in studies of genetic and nutritional iron deficiency. Blood *102*, 1893–1899.

Cherukuri, S., Tripoulas, N.A., Nurko, S., and Fox, P.L. (2004). Anemia and impaired stress-induced erythropoiesis in aceruloplasminemic mice. Blood Cells Mol. Dis. *33*, 346–355.

Dennis, J.E., Gay, D.M., and Welsch, R.E. (1981). Algorithm 573. NL2SOL — An adaptive nonlinear least-squares algorithm. ACM Trans. Math. Softw. *7*, 369–383.

Dini, L., Carbonaro, M., Musci, G., and Calabrese, L. (1990). The interaction of ceruloplasmin with Kupffer cells. Eur. J. Cell Biol. *52*, 207–212.

Donovan, A., Brownlie, A., Zhou, Y., Shepard, J., Pratt, S.J., Moynihan, J., Paw, B.H., Drejer, A., Barut, B., Zapata, A., et al. (2000). Positional cloning of zebrafish *ferroportin1* identifies a conserved vertebrate iron exporter. Nature *403*, 776–781.

Donovan, A., Lima, C.A., Pinkus, J.L., Pinkus, G.S., Zon, L.I., Robine, S., and Andrews, N.C. (2005). The iron exporter ferroportin/Slc40a1 is essential for iron homeostasis. Cell Metab. *1*, 191–200.

Dupic, F., Fruchon, S., Bensaid, M., Loreal, O., Brissot, P., Borot, N., Roth, M.P., and Coppin, H. (2002). Duodenal mRNA expression of iron related genes in response to iron loading and iron deficiency in four strains of mice. Gut *51*, 648–653.

Fleming, M.D., Trenor, C.C., Su, M.A., Foernzler, D., Beier, D.R., Dietrich, W.F., and Andrews, N.C. (1997). Microcytic anaemia mice have a mutation in *Nramp2*, a candidate iron transporter gene. Nat. Genet. *16*, 383–386.

Fleming, R.E., and Gitlin, J.D. (1990). Primary structure of rat ceruloplasmin and analysis of tissue-specific gene expression during development. J. Biol. Chem. *265*, 7701–7707.

Frazer, D.M., Vulpe, C.D., McKie, A.T., Wilkins, S.J., Trinder, D., Cleghorn, G.J., and Anderson, G.J. (2001). Cloning and gastrointestinal expression of rat hephaestin: relationship to other iron transport proteins. Am. J. Physiol. *281*, G931–G939.

Gunshin, H., Mackenzie, B., Berger, U.V., Gunshin, Y., Romero, M.F., Boron, W.F., Nussberger, S., Gollan, J.L., and Hediger, M.A. (1997). Cloning and characterization of a mammalian proton-coupled metal-ion transporter. Nature *388*, 482–488.

Gunshin, H., Starr, C.N., Direnzo, C., Fleming, M.D., Jin, J., Greer, E.L., Sellers, V.M., Galica, S.M., and Andrews, N.C. (2005). Cybrd1 (duodenal cytochrome b) is not necessary for dietary iron absorption in mice. Blood *106*, 2879–2883.

Hahn, P., Qian, Y., Dentchev, T., Chen, L., Beard, J., Harris, Z.L., and Dunaief, J.L. (2004). Disruption of ceruloplasmin and hephaestin in mice causes retinal iron overload and retinal degeneration with features of age-related macular degeneration. Proc. Natl. Acad. Sci. USA *101*, 13850–13855.

Harris, Z.L., Davis-Kaplan, S.R., Gitlin, J.D., and Kaplan, J. (2004). A fungal multicopper oxidase restores iron homeostasis in aceruloplasminemia. Blood *103*, 4672–4673.

Harris, Z.L., Durley, A.P., Man, T.K., and Gitlin, J.D. (1999). Targeted gene disruption reveals an essential role for ceruloplasmin in cellular iron efflux. Proc. Natl. Acad. Sci. USA *96*, 10812–10817.

Hellman, N.E., Schaefer, M., Gehrke, S., Stegen, P., Hoffman, W.J., Gitlin, J.D., and Stremmel, W. (2000). Hepatic iron overload in aceruloplasminaemia. Gut *47*, 858–860.

Hentze, M.W., Muckenthaler, M.U., and Andrews, N.C. (2004). Balancing acts: molecular control of mammalian iron metabolism. Cell *117*, 285–297.

Klebanoff, S.J. (1992). Bactericidal effect of Fe^{2+}, ceruloplasmin, and phosphate. Arch. Biochem. Biophys. *295*, 302–308.

Klomp, L.W.J., Farhangrazi, Z.S., Dugan, L.L., and Gitlin, J.D. (1996). Ceruloplasmin gene expression in the murine central nervous system. J. Clin. Invest. *98*, 207–215.

Kuo, Y.M., Su, T., Chen, H., Attieh, Z., Syed, B.A., McKie, A.T., Anderson, G.J., Gitschier, J., and Vulpe, C.D. (2004). Mislocalisation of hephaestin, a multicopper ferroxidase involved in basolateral intestinal iron transport, in the sex linked anaemia mouse. Gut *53*, 201–206.

Lockhart, P.J., and Mercer, J.F. (1999). Cloning and expression analysis of the sheep ceruloplasmin cDNA. Gene *236*, 251–257.

McKie, A.T., Barrow, D., Latunde-Dada, G.O., Rolfs, A., Sager, G., Mudaly, E., Mudaly, M., Richardson, C., Barlow, D., Bomford, A., et al. (2001). An iron-regulated ferric reductase associated with the absorption of dietary iron. Science *291*, 1755–1759.

McKie, A.T., Marciani, P., Rolfs, A., Brennan, K., Wehr, K., Barrow, D., Miret, S., Bomford, A., Peters, T.J., Farzaneh, F., et al. (2000). A novel duodenal iron-regulated transporter, IREG1, implicated in the basolateral transfer of iron to the circulation. Mol. Cell *5*, 299–309.

Nemeth, E., Tuttle, M.S., Powelson, J., Vaughn, M.B., Donovan, A., Ward, D.M., Ganz, T., and Kaplan, J. (2004). Hepcidin regulates cellular iron efflux by binding to ferroportin and inducing its internalization. Science *306*, 2090–2093.

Osaki, S., and Johnson, D.A. (1969). Mobilization of liver iron by ferroxidase (ceruloplasmin). J. Biol. Chem. *244*, 5757–5765.

Osaki, S., Johnson, D.A., and Frieden, E. (1966). The possible significance of the ferrous oxidase activity of ceruloplasmin in normal human serum. J. Biol. Chem. *241*, 2746–2751.

Patel, B.N., Dunn, R.J., Jeong, S.Y., Zhu, Q., Julien, J.P., and David, S. (2002). Ceruloplasmin regulates iron levels in the CNS and prevents free radical injury. J. Neurosci. *22*, 6578–6586.

Sarkar, J., Seshadri, V., Tripoulas, N.A., Ketterer, M.E., and Fox, P.L. (2003). Role of ceruloplasmin in macrophage iron efflux during hypoxia. J. Biol. Chem. *278*, 44018–44024.

Tavassoli, M., Kishimoto, T., and Kataoka, M. (1986). Liver endothelium mediates the hepatocyte's uptake of ceruloplasmin. J. Cell Biol. *102*, 1298–1303.

Torrance, J.D., and Bothwell, T.H., eds. (1980). Tissue iron stores (New York, Churchill Livingstone).

Vulpe, C.D., Kuo, Y.M., Murphy, T.L., Cowley, L., Askwith, C., Libina, N., Gitschier, J., and Anderson, G.J. (1999). Hephaestin, a ceruloplasmin homologue implicated in intestinal iron transport, is defective in the *sla* mouse. Nat. Genet. *21*, 195–199.

Yamamoto, K., Yoshida, K., Miyagoe, Y., Ishikawa, A., Hanaoka, K., Nomoto, S., Kaneko, K., Ikeda, S., and Takeda, S. (2002). Quantitative evaluation of expression of iron-metabolism genes in ceruloplasmin-deficient mice. Biochim. Biophys. Acta *1588*, 195–202.